DOI: 10.1002/ejoc.200900178

An Exhaustive Conformational Evaluation of the HIV-1 Inhibitor BMS-378806 through Theoretical Calculations and Nuclear Magnetic Resonance Spectroscopy

Diego Colombo,[a] Stefania Villa,[b] Lucrezia Solano,[b] Laura Legnani,[c] Franca Marinone Albini,[c] and Lucio Toma*[c]

Keywords: Molecular modeling / Density functional calculations / NMR spectroscopy / Antiviral agents / Nitrogen heterocycles

BMS-378806 (**1**) is an azaindole derivative known to interfere with the HIV-1 entry process by targeting the viral gp120 envelope glycoprotein and inhibiting its interaction to cellular CD4 receptors. To give a detailed comprehension of its conformational features, a theoretical study of **1** was performed at the B3LYP/6-31G(d) level of calculation. Tenths of populated conformations were located and grouped into four families corresponding to the possible arrangements at the two planar amido functions. In agreement with these results, the high-field ^{1}H NMR spectrum of **1**, recorded at 248 K, showed four distinct series of signals easily attributable to each family, thus confirming on experimental grounds the very high degree of conformational mobility of the compound.

Introduction

Currently used anti-HIV therapy is a combination cocktail of inhibitors of HIV reverse transcriptase and protease; it allows effective control of viral load and disease progression in HIV-infected individuals. Though this therapy has prolonged the survival of AIDS patients, the emergence of drug-resistant strains and the toxicity associated to the therapy have limited the efficacy of the current combination regimen. New drugs, with a different mechanism and improved anti-HIV potency, were studied as inhibitors that block HIV infection at the early stages. Indeed, a promising area of investigation is the identification of agents that inhibit viral attachment and entry into host cells.[1]

BMS-378806 (**1**), an azaindole derivative discovered at Bristol-Myers Squibb,[2] has been shown to interfere with the HIV-1 entry process by targeting the viral gp120 envelope glycoprotein and inhibiting its interaction with cellular CD4 receptors.[3] It was selective for HIV-1, specifically subtype B,[4] inactive against HIV-2, SIV, and a panel of other viruses.[3] The pharmacokinetic and pharmaceutical characteristics of BMS-378806 supported an oral formulation in man, and initial toxicology studies raised no safety concerns.[2,5] It was also being investigated in formulations for vaginal administration for the prevention of HIV-1 transmission when used in combination with other vaginal microbicides.[6]

The binding mode between **1** and HIV-1 gp120 was predicted by docking and molecular dynamics simulations[7] and was suggested to be similar to the binding of Phe43 in CD4. Actually, it was demonstrated that **1** inhibits the binding of gp120 to cellular CD4 receptors through a specific and competitive mechanism at a stoichiometry of approximately 1:1 with a binding affinity similar to that of soluble CD4. However, when the flexible molecular docking procedure combined with a molecular dynamics simulation was performed,[7] the structure of **1** was supposed to be rather rigid and only one rotatable bond was defined in the multiconformational docking, the one corresponding to the methoxy group at the 4-position of the azaindole ring, defined as τ_1 in Figure 1. Despite the apparent rigidity, BMS-378806 is a highly flexible molecule, as several other degrees of conformational freedom do exist: (i) the single bond between C3 of the azaindole and the adjacent carbonyl (τ_2); (ii) the vicinal dioxo system (τ_3); (iii) both the amido functions with the geometrical isomerism determined by the partial double bond character of the C–N bonds (τ_4 and τ_5); (iv) the single bond between the phenyl group and the adjacent carbonyl (τ_6); (v) the geometry of the piperazine ring (τ_7 and τ_8).

[a] Dipartimento di Chimica, Biochimica e Biotecnologie per la Medicina, Università di Milano,
Via Saldini 50, 20133 Milano, Italy
[b] Dipartimento di Scienze Farmaceutiche "Pietro Pratesi", Università di Milano,
Via Mangiagalli 25, 20133 Milano, Italy
[c] Dipartimento di Chimica Organica, Università di Pavia,
Via Taramelli 10, 27100 Pavia, Italy
Fax: +39-0382-987323
E-mail: lucio.toma@unipv.it

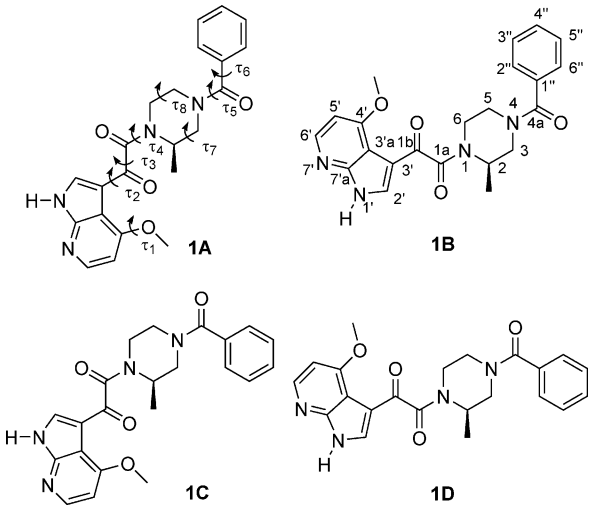

Figure 1. Conformational families of compound **1**.

In particular, the presence of the two amido functions and the height of the corresponding energy barriers to rotation allow four different arrangements to be distinguished on the NMR timescale (structures **1A**–**D**, Figure 1). Theoretical calculations can predict the relative stability of these four geometries and high-field ^{1}H NMR spectroscopy can give experimental proof of their individual existence. Thus, we performed a complete modeling study of BMS-378806 (**1**) at the B3LYP/6-31G(d) level[8] to determine all its accessible conformations. The result of the calculations was supported by high-field ^{1}H NMR experimental data.

Results and Discussion

The conformational properties of compound **1** were determined by optimization of all the possible starting geometries within the DFT approach at the B3LYP level with the 6-31G(d) basis set. Its conformational space was fully explored taking into consideration the various chair or twisted-boat conformations of the piperazine ring, the arrangement of the 1,2-dioxo system, the orientation at the bond between C3 of azaindole and the adjacent carbonyl group, and the orientation of the methoxy group at the 4-position of 7-azaindole and that of the phenyl in the benzoyl group. Moreover, as a result of the partial double bond character of the C–N bonds of the two amido functions, which makes the N–C=O systems almost planar, four different arrangements of these functional groups were considered.

Tenths of conformations were located and a number of them were populated. Their description has to be started from conformer **1Aa** (Figure 2), the global minimum geometry of **1**. As expected, in **1Aa** the piperazine ring assumes a chair conformation (τ_7 = 52° and τ_8 = –51°) and the C2 methyl group is axially oriented to avoid unfavorable steric interactions with the C1b carbon atom and/or the corresponding oxygen atom.

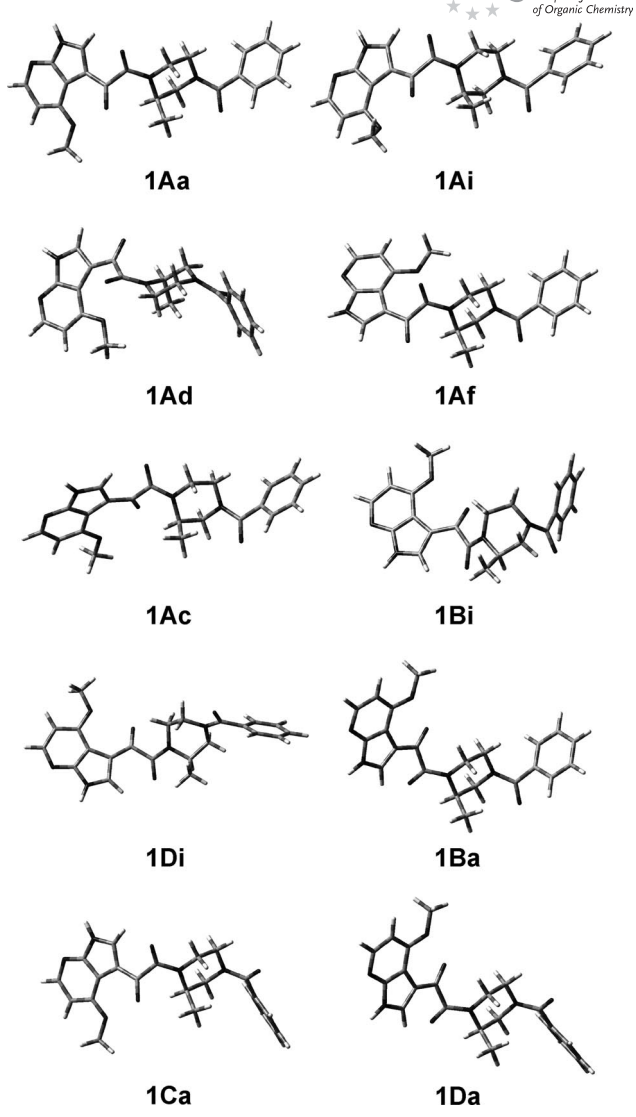

Figure 2. Three-dimensional plots of significant conformations of compound **1**.

The carbonyl oxygen atoms of the two amido functions point in opposite directions, with τ_4 (C2–N–C1a–C1b) close to 0° and τ_5 (C3–N–C4a–C1′′) close to 180° (this arrangement can be named "*anti*"). The two substituents of azaindole, that is, the C4′ methoxy and C1b carbonyl groups, lie on the plane of the heteroaromatic system with τ_1 (C3′a–C4′–O–CH_3) and τ_2 (C1a–C1b–C3′–C3′a) close to 180°. On the contrary, the dioxo system largely deviates from planarity with a value of –134° for τ_3 (N–C1a–C1b–C3′). On the other side of the molecule the same occurs for the benzoyl group with a value of –44° for τ_6 (N–C4a–C1′′–C2′′).

The numerous other conformations of compound **1** differ from **1Aa** in one or more geometrical features. Table 1 reports the relative energy, the equilibrium percentages at 248 K calculated through the Boltzmann equation, and selected geometrical data of all the conformers with a relative energy in a range of 3 kcal mol^{-1} above the global minimum, whereas Table 2 summarizes the percentage conformational preferences at each rotatable single bond.

Table 1. Relative energies [kcal mol^{-1}], equilibrium percentages at 248 K, and significant torsional angles[a] [°] of the conformations of compound **1**.

	E_{rel}	%	τ_1	τ_2	τ_3	τ_4	τ_5	τ_6	τ_7	τ_8
1Aa	0.00	10.1	178	168	–134	5	173	–44	52	–51
1Ab	0.11	8.1	178	170	–134	6	–176	44	53	–53
1Ac	0.25	6.1	–178	–171	133	–7	173	–44	53	–52
1Ad	0.58	3.1	175	–25	133	–12	173	–43	52	–52
1Ae	0.65	2.7	–178	–171	134	–8	–176	45	54	–53
1Af	1.00	1.3	–175	25	–136	10	173	–44	53	–50
1Ag	1.03	1.2	–176	25	–136	9	–176	43	53	–52
1Ah	1.24	0.8	174	–25	134	–14	–176	45	53	–53
1Ai	2.35	0.1	101	167	–134	6	172	–44	52	–52
1Aj	2.52	0.1	102	167	–134	5	–176	44	53	–53
1Ba	0.02	9.7	179	170	–135	–170	173	–44	52	–53
1Bb	0.49	3.7	178	171	–136	–170	–176	45	53	–54
1Bc	0.50	3.7	–178	–170	135	173	173	–44	52	–52
1Bd	0.60	3.0	–178	–169	135	173	–177	44	52	–53
1Be	1.07	1.1	–177	26	–138	–161	172	–43	53	–53
1Bf	1.41	0.6	176	–26	137	166	–176	43	52	–53
1Bg	1.50	0.5	175	–25	137	168	173	–44	51	–52
1Bh	1.65	0.4	–176	26	–139	–161	–176	46	53	–54
1Bi	2.02	0.2	178	172	–139	–169	–179	40	–38	–39
1Bj	2.37	0.1	99	168	–134	–172	173	–43	52	–53
1Ca	0.09	8.4	178	169	–134	5	28	44	52	–52
1Cb	0.35	5.0	178	173	–135	5	–32	–44	53	–53
1Cc	0.37	4.8	–178	–171	134	–6	28	43	53	–52
1Cd	0.76	2.1	173	–25	134	–12	31	42	52	–52
1Ce	0.96	1.4	–178	–170	134	–8	–31	–45	54	–53
1Cf	1.06	1.2	–175	25	–136	8	27	44	52	–51
1Cg	1.16	1.0	–175	25	–136	7	–33	–43	53	–52
1Ch	1.39	0.6	174	–25	135	–13	–31	–45	53	–53
1Ci	2.36	0.1	102	166	–135	4	28	43	52	–52
1Da	0.10	8.2	178	171	–135	–170	28	44	52	–53
1Db	0.48	3.8	–178	–169	135	172	27	44	52	–52
1Dc	0.67	2.6	179	171	–136	–172	–30	–45	53	–54
1Dd	0.76	2.2	–179	–171	135	172	–32	–44	53	–53
1De	1.27	0.8	–177	25	–138	–161	28	43	53	–53
1Df	1.61	0.4	176	–25	136	167	26	44	50	–52
1Dg	1.69	0.3	176	–25	136	166	–33	–43	52	–53
1Dh	1.99	0.2	180	28	–140	–162	–30	–46	53	–53
1Di	2.36	0.1	179	170	–139	–172	21	42	59	58
1Dj	2.47	0.1	178	172	–139	–170	25	45	–38	–40
1Dk	2.54	0.1	100	169	–135	–170	28	44	52	–53

[a] τ_1: C3a′–C4′–O–CH_3; τ_2: C3a′–C3′–C1b–C1a; τ_3: N1–C1a–C1b–C3′; τ_4: C2–N1–C1a–C1b; τ_5: C3–N4–C4a–C1′′; τ_6: N4–C4a–C1′′–C2′′; τ_7: N1–C2–C3–N4; τ_8: N1–C6–C5–N4.

Table 2. Conformational preferences [%] at 248 K of the rotatable single bonds of compound **1** defined by τ_1, τ_2, τ_3, and τ_6 for the overall ensemble of conformations and for each conformational family.

	τ_1		τ_2			τ_3		τ_6	
	180°	100°	180°	25°	–25°	–135°	135°	–45°	45°
Overall	99.5	0.5	84.1	7.2	8.4	63.9	36.1	49.1	50.9
A family	33.4	0.2	27.2	2.5	3.9	20.9	12.7	20.7	12.9
B family	22.9	0.1	20.4	1.5	1.1	15.2	7.8	15.1	7.9
C family	24.5	0.1	19.7	2.2	2.7	15.7	8.9	8.0	16.6
D family	18.7	0.1	17.1	1.0	0.7	12.1	6.7	5.3	13.5

An examination of the data in Table 1 shows that there is a large preference for values of τ_1 close to 180° (>99%), indicating that the methoxy group is oriented *anti* to C3′a. Actually, the energy profile, obtained from conformation **1Aa** through a complete rotation around the C4′–O bond, shows two other energy minima located at τ_1 = 101 and –93° with relative energy values of 2.35 and 3.42 kcal mol^{-1}, respectively, separated by a very small energy barrier from **1Aa**, whereas the highest barrier (7–8 kcal mol^{-1}) is located between them at τ_1 = 0°. These two other energy minima have the methyl group almost orthogonal to the azaindole system, as it can be seen from the 3D plot of **1Ai**, the most stable of them (Figure 2).

These data indicate that, though rotation is not forbidden, the methoxy group spends most of the time in the orientation with τ_1 ca. 180°. Instead, the C1b–C3′ bond was shown to have other populated minima. In fact, besides the arrangement with τ_2 close to 180°, conformational minima

with τ_2 values of –25 or 25° were observed that account, respectively, for 8.4 and 7.2% of the overall population (Table 2) and are separated from it by energy barriers of 7–9 kcal mol^{-1}. Conformations **1Ad** and **1Af** are examples of these kinds of arrangement.

The dioxo system showed two populated minima with values of τ_3 of –135 or 135° and a respective overall population of 63.9 and 36.1%. Interconversion between the two minima is very easy, as the barrier that passes through a planar arrangement with τ_3 = 180° has a height of only 3 kcal mol^{-1}. The benzoyl group shows a deviation of the phenyl group from planarity with respect the carbonyl group with two arrangements presenting values of τ_6 of –44 or 44°, which are almost isoenergetic as confirmed by the respective 49.1 and 50.9% overall population.

As far as the conformational mobility of the piperazine ring is concerned, modeling also allowed some conformations to be located that show this ring in the twisted-boat geometry; they are characterized by τ_7 and τ_8 values that are either both positive or both negative. However, their percentage contribution to the overall population was very low, as it can be seen, for example, from the data of **1Bi** and **1Di**, the two most stable of them, which are 2.02 and 2.36 kcal mol^{-1}, respectively, higher in energy than **1Aa**. Moreover, conformations with the inverted chair geometry, characterized by an equatorial arrangement of the C2 methyl group and by negative values of τ_7 and positive values of τ_8, were also located. The relative energy of the most stable one was >4 kcal mol^{-1}; so, the percentage contribution to the overall population can be considered negligible.

Finally, let us discuss the main conformational features of compound **1**, that is, the orientation around the two amido bonds defined by the torsional angles τ_4 and τ_5. In Table 1 all the located conformers are grouped into four families showing similar values of τ_4 and τ_5 and each family is defined by the upper case letter in the name of the conformation. Two families are characterized by an "*anti*" arrangement: family **A**, to which belongs the already mentioned global minimum **1Aa**, and family **D** with opposite values of τ_4 and τ_5, which are close to 180 and 0°, respectively. On the contrary, families **B** and **C** are characterized by a "*syn*" arrangement of the amido functions and show values of τ_4 and τ_5 that are close to 180 or 0°, respectively. In Figure 2, the lowest-energy conformers of the **B**, **C**, and **D** families are also reported, labeled as **1Ba**, **1Ca**, and **1Da**, respectively. All the families were significantly populated and summation of the percentages over the members of each family allowed their overall population to be determined as 33.6, 23.0, 24.6, and 18.8% for the **A**, **B**, **C**, and **D** families, respectively.[9] Then, we determined the energy barriers for the rotation around the amido N1–C1a and N4–C4a bonds; the computed height of the barriers was about 21 and 14 kcal mol^{-1}, respectively;[10] these values are high enough to give rise to distinguishable conformations on the NMR timescale.

At last, we computed the ^{1}H NMR chemical shifts for each populated conformation of compound **1** by using GIAO NMR calculations[11] at the same DFT B3LYP/6-31G(d) level already used for the optimizations. The obtained values were weighted averaged on the basis of the population percentages separately for the conformations of every family. The values for the hydrogen atoms of the piperazine ring are reported in Table 3 together with the corresponding experimental data (see below).

Table 3. B3LYP/6-31G(d) GIAO calculated ^{1}H NMR chemical shift (δ, in ppm relative to TMS) of the piperazine protons of compound **1** on the basis of the geometries optimized at the same level in comparison with the experimental values from the spectra recorded in CD_3OD.

	A family		**B** family		**C** family		**D** family	
	calcd.	exp.	calcd.	exp.	calcd.	exp.	calcd.	exp.
2	4.23	4.14	4.84	4.95	3.98	3.91	4.62	4.69
3ax	2.83	3.10	2.83	3.25	3.27	3.48	3.26	3.61
3eq	4.40	4.51	4.46	4.60	3.58	3.56	3.64	3.68
5ax	3.04	3.37	3.28	3.23	2.63	3.10	2.83	3.01
5eq	3.67	3.88	3.57	3.73	4.45	4.78	4.38	4.52
6ax	3.40	3.25	3.19	3.23	3.00	3.28	3.37	3.58
6eq	4.29	4.37	3.70	3.53	4.41	4.54	3.84	3.63

In order to give experimental support to the above theoretical results, compound **1** was synthesized according to the method reported in the literature[2] and its high-field ^{1}H NMR spectrum in [D_4]methanol was recorded. At 298 K it showed broad overlapped signals due to coalescence (see also ref.[2]); so, it was recorded at lower temperatures. In particular, the proton resonances had a good shape and resolution at 248 K, and this temperature was used for the study.

As expected, the spectrum was very complex and four distinct series of signals could be individuated through a careful study of the 1D and 2D COSY experiments, starting from the four well-resolved methyl doublets (J = 6.8 Hz; Figure 3). They correspond to the four conformational families predicted by the calculations. Also, comparing the relative ratio obtained from the integration of the methyl groups (26, 23, 30, and 21% from the upfield to the downfield signal) with that calculated for the overall population of the four conformational families (see before),[12] and the experimental versus calculated chemical shifts of the piperazine protons as reported in Table 3, it was possible to assign the 1.17, 1.23, 1.35, and 1.40 ppm resonances to the methyl groups of the **1C**, **1D**, **1A**, and **1B** families, respectively. On the basis of the above-reported methyl resonances, four corresponding H-2 piperazine protons were assigned at 3.91 (**1C**), 4.14 (**1A**), 4.69 (**1D**), and 4.95 (**1B**) ppm, respectively (see Table 3), as broad multiplets. Consequently also the H-3 axial/equatorial protons were assigned at 3.48/3.56 (**1C**), 3.10/4.51 (**1A**), 3.61/3.68 (**1D**), and 3.25/4.60 (**1B**) ppm (Table 3) as multiplets and broad doublets (J = 13.5 Hz), respectively. A cross peak due to the long range "W" coupling between the equatorial H-3 and H-5 piperazine protons confirmed the assignment of the configuration of the geminal H-3 protons. Consequently, the four couples of H-5 axial/equatorial protons were also assigned at 3.10/4.78 (**1C**), 3.37/3.88 (**1A**), 3.01/4.52 (**1D**), and 3.23/3.73 (**1B**) ppm

(Table 3) with J = 12.5, 12.5, and 4.0 Hz for the ddd axial and 12.5 Hz for the broad doublet equatorial H-5 protons. The H-6 axial/equatorial protons of the piperazine ring were assigned as multiplets/broad doublets (J = 12.5 Hz) at 3.28/4.54 (**1C**), 3.25/4.37 (**1A**), 3.58/3.63 (**1D**), and 3.23/3.53 (**1B**) ppm by comparing the experimental and calculated chemical shift values (Table 3). Also, the azaindole protons could be assigned under these experimental conditions: four singlets at 8.20, 8.22, 2.28, and 8.31 ppm accounting in particular for the H-2′ resonances. Four doublets at 8.23, 8.23, 8.25, and 8.25 ppm (J = 5.8 Hz) and at 6.93, 6.93, 6.95, and 6.95 ppm (J = 5.8 Hz) were referred to the H-6′ and H-5′ protons. In these cases, it was not possible to relate the chemical shifts to the conformational families **1A**–**D** as a result of the overlap of the resonances, but the four methoxy singlets at 4.01, 4.02, 4.03, and 4.04 ppm were tentatively assigned as the **1C**, **1D**, **1A**, and **1B** conformers, respectively, on the basis of their integration. Finally, a multiplet at 7.40–7.56 ppm accounted for the five benzoyl protons of BMS-378806.

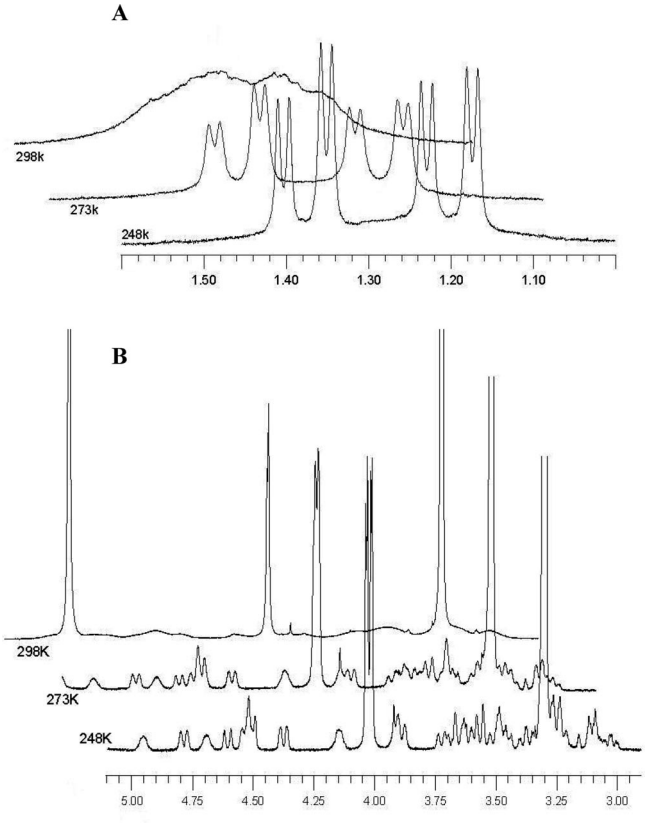

Figure 3. ^{1}H NMR spectra of compound **1** at 248, 273, and 298 K. **A**: signals of the C2 methyl group; **B**: signals of the piperazine hydrogen atoms and the methoxy group.

Conclusions

A theoretical conformational evaluation of BMS-378806 was performed; it allowed tenths of populated conformations that differ in the orientation at the several rotatable single bonds as well as in the conformation of the piperazine ring to be located. The conformations were grouped into four families corresponding to the possible arrangements at the two planar amido functions. The high-field ^{1}H NMR spectrum of **1**, recorded in [D_4]methanol at 248 K, showed four distinct series of signals easily attributable to each of the conformational families predicted by the calculations. These results show that BMS-378806 presents a very high degree of conformational flexibility. As it is well known that the active conformation of a ligand might be neither the global minimum nor a low energy one, none of the located conformations can be, in principle, neglected in the evaluation of the binding mode of **1** to a proteic partner.

Methods

Theoretical Calculations: A systematic search of the conformational space of compound **1** was performed by using the Gaussian03 program package[13] through optimizations in the gas phase at the B3LYP/6-31G(d) level. First, a starting geometry presenting the **A** arrangement at the amido functions and the chair conformation of the piperazine ring was optimized. Then, the energy profiles for rotation around the single bonds defined by τ_1, τ_2, τ_3, and τ_6 were determined with a step size of 30°. All the combinations of the $3 \times 3 \times 2 \times 2$ observed minima were used to generate 36 starting geometries optimized as above. The procedure was similarly repeated for the **B**, **C**, and **D** arrangements as well as for the inverted chair and twisted-boat geometries of the piperazine ring. Vibrational frequencies were computed at the same level of theory to verify that the optimized structures were minima. Thermodynamics allowed the enthalpies and the Gibbs free energies to be calculated. The solvent effects were considered by single-point calculations, in water and in methanol, at the same level as above, on the gas-phase optimized geometries by using a self-consistent reaction field (SCRF) method based on the polarizable continuum model (PCM).[14] The population percentages were calculated through the Boltzmann equation at 248 K. GIAO NMR calculations[11] were carried out at the B3LYP/6-31G(d) level.

NMR Spectroscopy: All NMR spectra were recorded with a Bruker Avance-500 spectrometer operating at 500.13 MHz for ^{1}H by using a 5 mm z-PFG (pulsed field gradient) broadband reverse probe at different temperatures obtained through a Bruker BVT 3000 digital temperature control unit connected at a liquid nitrogen evaporator system. Chemical shifts are reported on the δ (ppm) scale and are relative to residual methanol signals (δ =3.30 ppm), and scalar coupling constants are reported in Hertz. The data were collected and processed by XWIN-NMR software (Bruker) running on a PC with Microsoft Windows XP. Compound **1** (3.5 mg) was dissolved in CD_3OD (0.6 mL) and put in a 5-mm NMR tube. The signal assignments were given by a combination of 1D and 2D experiments by using standard Bruker pulse programs. The ^{1}H–^{1}H bond correlations were confirmed by COSY experiments by using Z-PFGs. The pulse widths were 7.15 μs (90°) for ^{1}H. Typically, 32 K data points were collected for 1D spectra. Spectral widths were 11.45 ppm (5733 Hz) for ^{1}H NMR (digital resolution: 0.17 Hz per point). 2D experiments parameters were as follows. For ^{1}H–^{1}H correlations: relaxation delay 2.0 s, data matrix 1 K × 1 K (512 experiments to 1 K zero filling in F_1, 1 K in F_2), 2 transients in each experiment for COSY, spectral width 8.5 ppm (4250.0 Hz). A sinebell weighting was applied to each dimension. All 2D spectra were processed with the Bruker software package.

Acknowledgments

The authors acknowledge the financial support from the University of Pavia and the University of Milano. They also thank CILEA for the allocation of computer time.

[1] a) V. Briz, E. Poveda, V. Soriano, *J. Antimicrob. Chemother.* **2006**, *57*, 619–627; b) S. Rusconi, A. Scozzafava, A. Mastrolorenzo, C. T. Supuran, *Curr. Drug Targets Infect. Disord.* **2004**, *4*, 339–355; c) F. Shaheen, R. G. Collman, *Curr. Opin. Infect. Dis.* **2004**, *17*, 7–16; d) I. Markovic, *Curr. Pharm. Des.* **2006**, *12*, 1105–1119.

[2] T. Wang, Z. Zhang, O. B. Wallace, M. Deshpande, H. Fang, Z. Yang, L. M. Zadjura, D. L. Tweedie, S. Huang, F. Zhao, S. Ranadive, B. S. Robinson, Y. F. Gong, K. Ricarrdi, T. P. Spicer, C. Deminie, R. Rose, H. G. H. Wang, W. S. Blair, P. Y. Shi, P. F. Lin, R. J. Colonno, N. A. Meanwell, *J. Med. Chem.* **2003**, *46*, 4236–4239.

[3] P. F. Lin, W. Blair, T. Wang, T. Spicer, Q. Guo, N. Zhou, Y. F. Gong, H. G. H. Wang, R. Rose, G. Yamanaka, B. Robinson, C. B. Li, R. Fridell, C. Deminie, G. Demers, Z. Yang, L. Zadjura, N. Meanwell, R. Colonno, *Proc. Natl. Acad. Sci. USA* **2003**, *100*, 11013–11018.

[4] P. L. Moore, T. Cilliers, L. Morris, *AIDS* **2004**, *18*, 2327–2330.

[5] Z. Yang, L. Zadjura, C. D'Arienzo, A. Marino, K. Santone, L. Klunk, D. Greene, P. F. Lin, R. Colonno, T. Wang, N. Meanwell, S. Hansel, *Biopharm. Drug Dispos.* **2005**, *26*, 387–402.

[6] R. S. Veazey, P. J. Klasse, S. M. Schader, Q. Hu, T. J. Ketas, M. Lu, P. A. Marx, J. Dufour, R. J. Colonno, R. J. Shattock, M. S. Springer, J. P. Moore, *Nature* **2005**, *438*, 99–102.

[7] R. Kong, J. J. Tan, X. H. Ma, W. Z. Chen, C. X. Wang, *Biochim. Biophys. Acta* **2006**, *1764*, 766–772.

[8] a) A. D. Becke, *J. Chem. Phys.* **1993**, *98*, 5648–5652; b) C. Lee, W. Yang, R. G. Parr, *Phys. Rev. B* **1988**, *37*, 785.

[9] Frequency calculations on all the conformations allowed the H and G corrections to energy values to be determined. The overall population of each conformational family, recalculated on the basis of the ΔH values, was 33.6, 23.3, 25.6, and 17.5% for the **A**, **B**, **C**, and **D** families, respectively. The corresponding percentages calculated by using the ΔG values were 22.7, 34.3, 17.9, and 25.1%.

[10] These values are in agreement with data reported in the literature for *N*,*N*-dialkylamides. See for example: A. Rauk, *J. Org. Chem.* **1996**, *61*, 2337–2345. For a review on hindered rotation in amides, see: W. E. Stewart, T. H. Siddall, *Chem. Rev.* **1970**, *5*, 517–551.

[11] a) K. Wolinski, F. James, J. F. Hinton, P. Pulay, *J. Am. Chem. Soc.* **1990**, *112*, 8251–8260; b) R. Ditchfield, *Mol. Phys.* **1974**, *27*, 789–807.

[12] The energy of the conformations optimized in vacuo was recalculated by using a polarizable continuum model (PCM) by choosing water and methanol as the solvents. The overall population of each conformational family, recalculated in water, was 40.3, 18.0, 27.5, and 14.2% for the **A**, **B**, **C**, and **D** families, respectively. The corresponding percentages in methanol were 39.1, 18.0, 26.3, and 16.7%.

[13] M. J. Frisch, G. W. Trucks, H. B. Schlegel, G. E. Scuseria, M. A. Robb, J. R. Cheeseman, J. A. Montgomery Jr, T. Vreven, K. N. Kudin, J. C. Burant, J. M. Millam, S. S. Iyengar, J. Tomasi, V. Barone, B. Mennucci, M. Cossi, G. Scalmani, N. Rega, G. A. Petersson, H. Nakatsuji, M. Hada, M. Ehara, K. Toyota, R. Fukuda, J. Hasegawa, M. Ishida, T. Nakajima, Y. Honda, O. Kitao, H. Nakai, M. Klene, X. Li, J. E. Knox, H. P. Hratchian, J. B. Cross, C. Adamo, J. Jaramillo, R. Gomperts, R. E. Stratmann, O. Yazyev, A. J. Austin, R. Cammi, C. Pomelli, J. W. Ochterski, P. Y. Ayala, K. Morokuma, G. A. Voth, P. Salvador, J. J. Dannenberg, V. G. Zakrzewski, S. Dapprich, A. D. Daniels, M. C. Strain, O. Farkas, D. K. Malick, A. D. Rabuck, K. Raghavachari, J. B. Foresman, J. V. Ortiz, Q. Cui, A. G. Baboul, S. Clifford, J. Cioslowski, B. B. Stefanov, G. Liu, A. Liashenko, P. Piskorz, I. Komaromi, R. L. Martin, D. J. Fox, T. Keith, M. A. Al-Laham, C. Y. Peng, A. Nanayakkara, M. Challacombe, P. M. W. Gill, B. Johnson, W. Chen, M. W. Wong, C. Gonzalez, J. A. Pople, *Gaussian 03*, Revision B.04, Gaussian, Inc., Pittsburgh, PA, **2003**.

[14] a) E. Cances, B. Mennucci, J. Tomasi, *J. Chem. Phys.* **1997**, *107*, 3032–3042; b) M. Cossi, V. Barone, R. Cammi, J. Tomasi, *Chem. Phys. Lett.* **1996**, *255*, 327–335.

Received: February 19, 2009
Published Online: May 13, 2009

